DENOISING SONAR IMAGES USING A BISHRINK FILTER WITH REDUCED SENSITIVITY

ALEXANDRU ISAR[1], SORIN MOGA[2], DORINA ISAR[1]

Key words: SONAR, MAP-filter, Double Tree Complex Wavelet Transform (DT-CWT), Sensitivity.

The SAR and SAS images are perturbed by a multiplicative noise called speckle, due to the coherent nature of the scattering phenomenon. This paper presents a new denoising method in the wavelet domain, which tends to reduce the speckle, preserving the structural features (like the discontinuities) and textural information of the scene. Due to the massive proliferation of SONAR images, the proposed technique is very appealing in ocean applications. In fact it is a pre-treatment required in any SONAR images analysis system. In this paper we propose the adaptation to the case of speckle noise of a denoising method developed by the authors in the case of additive white Gaussian noise. It is simple and fast. Some simulation results and comparisons prove the performance of the new algorithm.

1. **INTRODUCTION**

The SONAR images represent a particular case of Synthetic Aperture Radar (SAR) images. The SAR images are perturbed by a noise named speckle. It is of multiplicative nature. The aim of a denoising algorithm is to reduce the noise level, while preserving the image features. There are a lot of references treating the denoising of SAR images, but the particular case of SONAR images is analyzed in a very small number of papers, despite their specificities. A first particularity of SONAR images is their potential low quality. Depending on the acquisition conditions, the Signal to Noise Ratio (SNR) of SONAR images can be very low. A second particularity of the SONAR images is that they contain almost homogeneous and textured regions. The presence of edges in a SONAR image is relatively rare. The multiplicative speckle noise that perturbs the SONAR images can be transformed into an additive noise with the aid of a logarithm computation block. At the end, to obtain the denoising result, the logarithm inversion is

[1] "Politehnica" University of Timişoara, E-mail: alexandru.isar@etc.upt.ro.
[2] Telecom Bretagne, Brest, France.

performed. A potential architecture for a SONAR denoising system is presented in Fig. 1.

The denoising system must contain a mean correction block. The corresponding block in Fig. 1 computes the mean of the acquired image (which is equal with the mean of its noise-free component because the speckle noise has unitary mean) and corrects the mean of the result (the mean of the image at the output of the block that invert the logarithm is extracted and the mean of the acquired image is added). The first goal of this paper is the additive noise denoising kernel. The most straightforward way of distinguishing information from noise in the wavelet domain consists of thresholding the wavelet coefficients. Soft-thresholding is the most popular strategy and has been theoretically justified by Donoho and Johnstone, [1]. They propose a three steps denoising algorithm:

1. the computation of a forward WT,
2. the filtering with a non-linear filter,
3. the computation of the corresponding inverse wavelet transform (IWT).

They use the Discrete Wavelet Transform (DWT) and the soft-thresholding filter. They do not make any explicit hypothesis on the noise-free image. Their unique statistical hypothesis refers to the noise, considered additive white and Gaussian, (AWGN). The soft–thresholding filter puts to zero all the wavelet coefficients with the absolute value smaller then a threshold. This threshold is selected to minimize the min-max approximation error. The soft-thresholding filter was enhanced in [2]. Some relatively recent research has addressed the development of statistical models of wavelet coefficients of natural images and application of these models to image denoising. The corresponding signal processing treatments can be considered as parametric denoising methods. Highly effective yet simple schemes mostly based on soft-thresholding have been developed [3, 4]. An appealing particularity of the WTs is the inter-scale dependence. If at a given scale a coefficient is large, its correspondent at the next scale (having the same spatial coordinates) will be also large. In [2–4] the inter-scale dependencies are used to improve the denoising performance. The wavelet coefficients statistical models which exploit the dependence between coefficients give better results compared to the ones using an independent

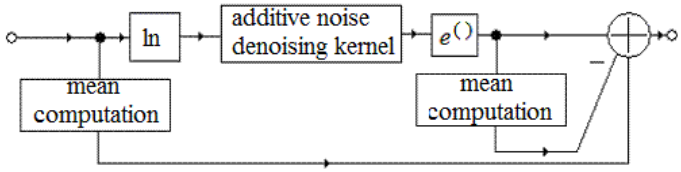

Fig. 1 – The architecture of the proposed denoising system. The mean correction mechanism and the kernel are highlighted.

assumption [5, 6]. The denoising is performed in [5] and [6] with the aid of maximum a posteriori filters, (MAP). The filter in [5] is named bishrink filter. The denoising performance of MAP filters can be improved with the aid of two-stage denoising system. The first stage treats the acquired image furnishing a pilot for the second stage. The acquired image is once again treated by the second stage but this time the information carried by the pilot is used. The idea of two-stage denoising systems was introduced in [7]. Another two-stage denoising algorithms applied to images was proposed in [8]. A very nice contribution of [8] is the idea of directional windows. The rectangular windows used for the estimation of the local variance of the clean image are replaced by elliptical windows oriented following the preferential direction of the current detail sub-image. This is a first example of exploiting the intra-scale dependence of the wavelet coefficients. The aim of [9] was to correct the comportment of the bishrink filter in the homogeneous regions of very noisy images. The goal of this paper is to apply the denoising system proposed in [9] to the case of SONAR images. The structure of this paper is the following. In the second paragraph is recalled the denoising algorithm proposed in [9]. The third paragraph is dedicated to the presentation of the simulation results and to some comparisons with the best available wavelet based SONAR images denoising results conceived to illustrate the effectiveness of the proposed algorithm. The paper's conclusion is formulated in the fifth paragraph.

2. **A DENOISING SYSTEM WITH REDUCED SENSITIVITY**

In [9] was proved that when the value of the estimation of the noise standard deviation is higher then the performance of the bishrink filter is poorer. One of the goals of this paper was to correct this comportment. In the same paper was already proved that the bishrink filter treats very well the edges, the estimation of the textured regions must be corrected and the worst treatment corresponds to the homogeneous regions. In consequence the most difficult regime of the bishrink filter corresponds to the treatment of homogeneous regions of very noisy images. The denoising system proposed in [9] corrects this comportment based on the diversification principle. This concept was used in [15, 17] to improve the denoising of SAR and SONAR images. The final estimate in [9] is obtained by fusion of six partial results. Inspired by [10] the fusion technique selected in [9] was the averaging. Another very interesting fusion technique, based on the use of the multi-wavelet discrete wavelet transform, is proposed in [12]. The architecture of the denoising kernel proposed in [9] is presented in Fig. 2.

The first stage of the algorithm contains the blocks: DT-CWT_A, F_2, IDTCWT_A and Segm. The second one contains the other blocks. Two types of WT, DT-CWT_A and DT-CWT_B are computed obtaining the wavelet coefficients w_A

and w_B. Three variants of bishrink filter, F_1-the genuine one, F_2-the adaptive bishrink filter with global estimation of the local variance and F_3-the mixed bishrink filter, are applied in the field of each DT-CWT. Six estimates of wavelet coefficients $\hat{w}_{1A}$, $\hat{w}_{2A}$, $\hat{w}_{3A}$, $\hat{w}_{1F}$, $\hat{w}_{2F}$ and $\hat{w}_{3F}$, are obtained. For each one the inverse WT, IDT-CWT, is computed, obtaining six partial results, $\hat{s}_{1A}$, $\hat{s}_{2A}$, $\hat{s}_{3A}$, $\hat{s}_{1F}$, $\hat{s}_{2F}$ and $\hat{s}_{3F}$. The image $\hat{s}_{2A}$ is segmented in six classes following the values of the local variances of its pixels obtaining the pilot image. Registering the coordinates of the pixels belonging at each of these classes the six masks are generated. With the aid of these masks the six classes, of each partial result are identified. Using the class selectors CS1-CS6, each partial result is treated in a different manner. The segmentation block, Segm, creates the six masks. Each mask is used by the corresponding CS. These systems pick up the pixels of their input images with the coordinates belonging to the correspondent mask, generating each class of the partial results. CS1 has only one input and generates with the aid of the sixth mask the first class of the image $\hat{s}_{2A}$. CS2 has two inputs and generates with the aid of the fifth mask the second classes of the partial results $\hat{s}_{2A}$ and $\hat{s}_{3A}$ and so on. The first class of the final estimate $\hat{s}_1$ is identical with the first class of the image $\hat{s}_{2A}$. The image $\hat{s}_{2A}$ is segmented in classes which elements have a value of the local variance $\hat{\sigma}_{2A}$, belonging to one of six possible intervals:

$$I_p = \left(\alpha_p \hat{\sigma}_{2A\max}, \alpha_{p+1} \hat{\sigma}_{2A\max}\right)_{1\le p\le 6},$$

where $\alpha_1 = 0$ and $\alpha_7 = 1$. The class selector CS_p in Fig. 2 selects the class associated to the interval I_{7-p}. In [9] were proposed the following values for the bounds of the intervals I_p: $\alpha_2 = 0.025, \alpha_3 = 0.05$, $\alpha_4 = 0.075$, $\alpha_5 = 0.1$ and $\alpha_6 = 0.25$.

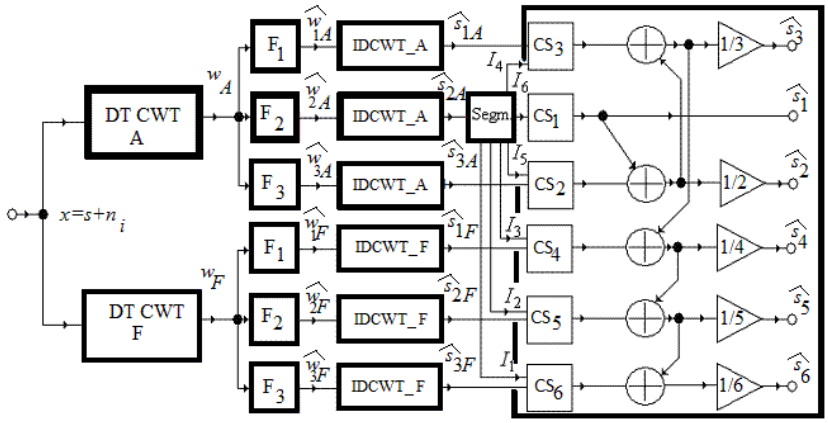

Fig. 2 – The architecture of the proposed additive noise denoising kernel.

3. **SIMULATION RESULTS**

We present two types of simulation results: for synthesized speckle noise and for real SONAR images.

3.1. SPECKLE SYNTHESIZED

In this case the noise is generated following a Rayleigh distribution and has a multiplicative nature. For the case of the image Lena the result presented in Fig. 3 was obtained. The PSNR gain performed by the proposed method is in this case of 10 dB, equivalent with the performance obtained applying the SAR denoising method proposed in [13]. The two denoising algorithms proposed in [13] use the UDWT. It is computed either with the aid of the Daubechies mother wavelets with eight vanishing moments (db8) or with the pair of biorthogonal mother wavelets Daubechies 9 and Daubechies 7 (bior9.7). The first denoising algorithm proposed in [13] performs a local linear minimum mean square error (LLMMSE) filtering in the UDWT domain. The second one uses a MAP filter constructed supposing that the noise-free wavelet coefficients and the wavelet coefficients of the noise are distributed following Generalized Gaussian Distributions. The parameters of those probability density function (pdfs) are estimated for each pixel of the input image. The corresponding MAP filter equation is solved with the aid of numerical methods. A detailed comparison of the denoising method in [13] and the proposed denoising method from the PSNR enhancement is presented in Table 1. The proposed denoising method performs better for noisier images. An excellent criterion for the appreciation of the quality of a denoising method conceived for the reduction of the multiplicative noise is based on the computation of the method noise. It represents the ratio of the noisy image by the denoising result, [14]. The method noise must be identical with the input noise for a perfect denoising method. It can be observed, analyzing Fig. 3, that the input noise (represented in the second picture from the first column) has the same aspect like the method noise (represented in the second picture from the second column). There are some fine differences between the images of the input noise and of the method noise, observable especially in the dark regions of the noise-free component of the input image (represented in the first picture of the first line in Fig. 3). In the last picture from the second line of Fig. 3 is carried-out a comparison between the histograms of the input noise (up) and of the method noise (bottom), highlighting the statistical differences between these two noises.

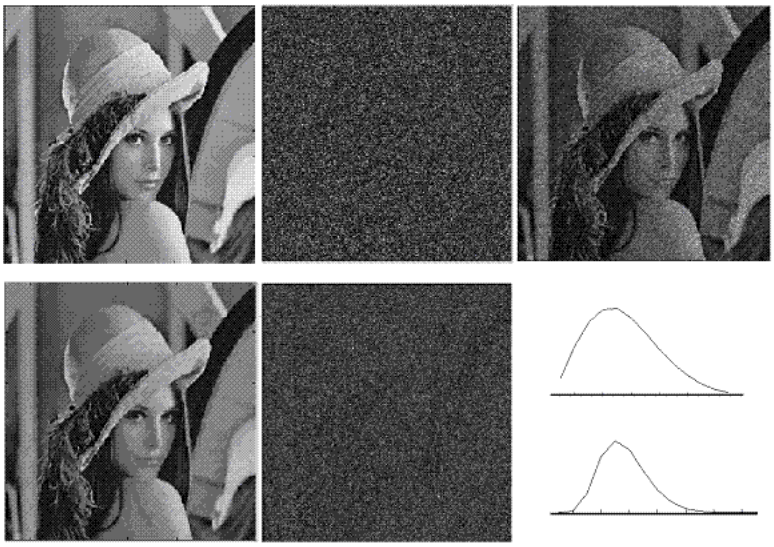

Fig. 3 – Synthesized speckle noise. First line, from left to right: clean image; synthesized speckle; noisy image (PSNR = 21.4 dB). Second line, from left to right: denoised image (PSNR = 31.4 dB); method noise; histograms of the noise (up) and method noise (bottom).

They are distributed following the same type of law (a Rayleigh law), but the input noise has a higher variance. It means that the contrast of the noise-free input image is affected by the proposed denoising method.

A comparison of the proposed method with the classical speckle removing methods proposed by: Lee, Frost and Kuan and with the wavelets based method from [10] and [11], for the example in Fig. 3, is presented in Table 2. In the case of the classical speckle removing methods, rectangular estimation windows with size 7×7 were used. From the PSNR point of view the method proposed in this paper has the best performance between those compared in Table 2. The proposed method makes a good treatment of edges and of homogeneous regions. Its drawback is the textures treatment, some of the fine textures of the clean component of the acquired image being erased by the denoising. A better analysis of the visual aspect of the proposed method can be carried out if it is applied to the test image proposed in [16], which consist of a collection of six synthetic and real sub-images. The sub-images 1, 5 and 6 represent real scenes. The sub-image 2 contains three types of synthesized textures and the sub-image 4 contains some synthesized homogeneous regions and contours. The sub-image 3 represents a zone of the image Lena. A comparison of denoising methods is presented in Fig. 4, based on the sub-images: 2, 3 and 4.

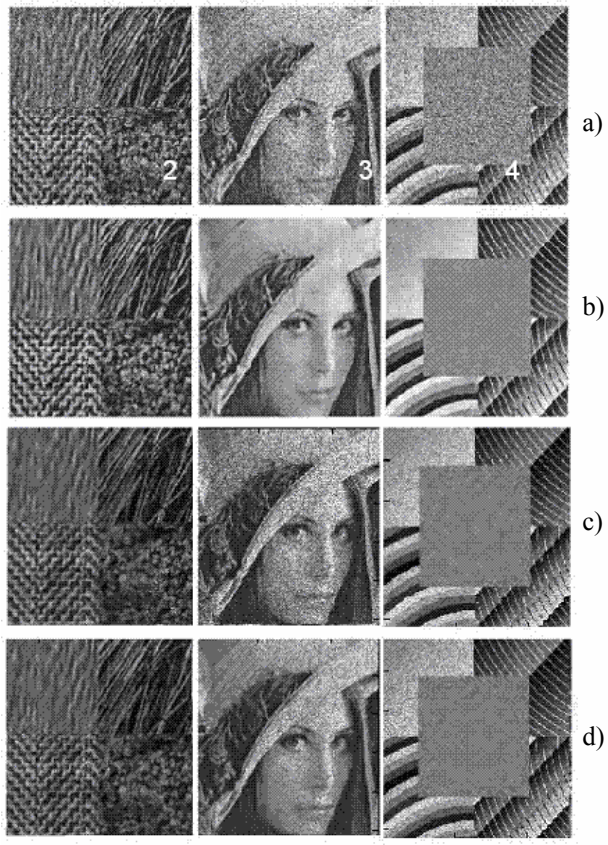

Fig. 4 – From up to bottom: a) noisy sub-images; b) results obtained in [16]; c) results obtained applying the method proposed in [11]; d) results of the proposed denoising method.

Table 1

A comparison between the speckle reduction methods described in [13] and the proposed method

	Raw	LLMMSE-UWD [13]		MAP-UWD [13]		Proposed
		dB8	bior9.7	dB8	bior9.7	
1-look	12.1	24.2	24.2	26.0	26.2	**26.4**
4-look	17.8	28.2	28.3	29.4	*29.6*	**29.9**
16-look	23.7	32.2	32.4	*32.9*	**33.0**	32.2

Table 2

The PSNR of different speckle denoising methods (in dB)

Noisy	Lee	Frost	Kuan	[10]	[11]	Proposed
21.4	27.2	27.03	28.12	28.56	29.63	31.4

The methods from [11] and [16] are compared with the proposed denoising method. The better treatment of the homogeneous regions is carried-out by the pure statistical method in [16] but it erases some contours and textures carrying-out an over-smooth filtering. The other two methods use the DT-CWT and treat better the details. The method proposed in [11], based on the DT-CWT-genuine bishrink filter denoising association does not eliminate all the noise. This effect is easy visible in the homogeneous regions. The proposed denoising method makes a good treatment of real scenes, eliminating completely the noise and introducing small distortions.

3.2. **REAL SONAR IMAGES**

Fig. 5 shows the original SONAR image "Swansea" and the results obtained with the method in [10] and the proposed method.

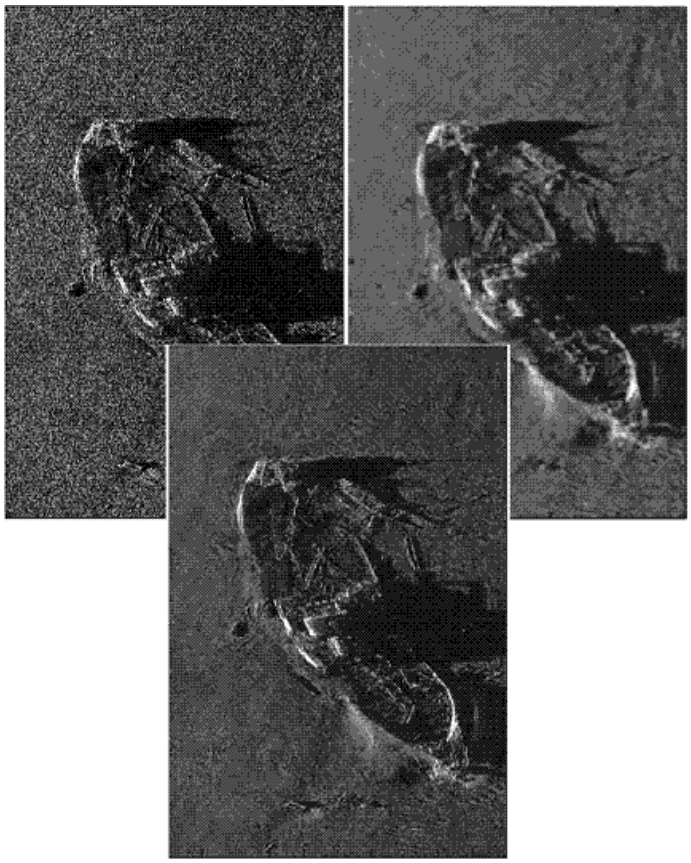

Fig. 5 – Speckle removal for the sea-bed sonar image Swansea (we are thankful to GESMA for providing this image). First line, left: acquired image (ENL=3.4); right: result in [10] (ENL=106). Second line: proposed method denoising result (ENL=101.8). The result in [10] looks over-smoothed. This comportment explains the small ENL reduction in the case of the proposed method.

The visual analysis of the filtered image proves the correctness of our assumptions. Indeed the result of the proposed method has a better visual aspect, the result in [10] being slightly over-smoothed. An objective measure of the homogeneity degree of a region was proposed for SAR images and is named enhancement of the Equivalent Number of Looks (ENL). It is defined by the ratio of the square of the mean and the variance of the pixels situated in the considered region. The enhancement of the ENL of a denoising method in a homogeneous region is defined by the ratio of the ENLs of the considered region computed before and after the application of the method. The performance obtained for homogeneous regions by the proposed denoising method is certificated by the important enhancement of the ENL obtained considering a region of 120×1000 pixels.

4. **CONCLUSION**

This paper presents an effective image denoising algorithm for SONAR images. It is based on an additive noise denoising kernel recently proposed in [9] that improves the treatment of homogeneous zones for very noisy images. We presented our simulation results and compared with published results in order to illustrate the effectiveness of the proposed algorithm. The comparisons suggest that the results obtained are competitive with the best results reported in the literature both for SAR and SONAR images denoising. One of our future research works will be the inclusion in the proposed algorithm of the intra-scale dependence of wavelet coefficients information. We believe that the idea of directional estimation windows proposed in [8] is a good candidate for this task. Another possible solution is the consideration of the phase information provided by the DT-CWT in a similar manner like that very recently proposed by Kingsbury [17], in association with the BLS-GSM algorithm. The research of new diversification mechanisms and of new synthesis techniques, like for example that proposed in [12], will represent other future directions for our team.

ACKNOWLEDGEMENTS

We have established collaboration with the specialists from the French Sea Institute, IFREMER, from Brest, with respect to the denoising of SONAR images. We acknowledge the importance of many hours spent in meetings with Xavier Lurton and Jean-Marie Augustin dedicated to our introduction in SONAR technology. This research was funded by a grant from CNCSIS, ID_930, with the title Using wavelet theory for decision making.

Received on November 11, 2008

REFERENCES

1. D. L. Donoho, I. M. Johnstone, *Adapting to unknown smoothness via wavelet shrinkage*, J. Amer. Statist. Assoc., **90**, *432*, pp. 1200–1224, Dec. 1995.
2. F. Luisier, T. Blu, M. Unser, *A New SURE Approach to Image Denoising: Interscale Orthonormal Wavelet Thresholding*, IEEE Transactions on Image Processing, **16**, *3*, pp. 593-606, March 2007.
3. Z. Cai, T. H. Cheng, C. Lu, K. R. Subramanian, *Efficient wavelet-based image denoising algorithm*, Electronics Letters, **37**, *11*, pp. 683-685, May 2001.
4. S. Chang, B. Yu, M. Vetterli, *Adaptive wavelet thresholding for image denoising and compression*, IEEE Transactions on Image Processing, **9**, *9*, pp. 1522-1531, 2000.
5. L. Sendur, I. W. Selesnick, *Bivariate shrinkage with local variance estimation*, IEEE Signal Processing Letters, **9**, *12*, pp. 438-441, December 2002.
6. A. Achim, E. E. Kuruoglu, *Image Denoising Using Bivariate α-stable Distributions in the Complex Wavelet Domain*, IEEE Signal Processing Letters, **12**, *1*, pp. 17-20, January 2005.
7. S. P. Ghael, A. M. Sayeed, R. G. Baraniuk, *Improved Wavelet Denoising via Empirical Wiener Filtering*, Proceedings of SPIE, *Mathematical Imaging*, San Diego, July, 1997.
8. P.-L. Shui, *Image Denoising Algorithm via Doubly Local Wiener Filtering with Directional Windows in Wavelet Domain*, IEEE Signal Processing Letters, **12**, *10*, pp. 681-684, October 2005.
9. A. Isar, S. Moga, D. Isar, *Denoising Images Using A New Type Of Bishrink Filter,* submitted to Rev. Roum. Sci. Techn. – Électrotechn. et Énerg.
10. A. Isar, D. Isar and A. Quinquis, *Multi-Scale MAP Denoising of SAR and SAS Images*, Sea Technology, **48**, *2*, pp. 46-48, February 2007.
11. R. Fablet, J.-M. Augustin, *Variational Multiwavelet Restoration of Noisy Images*, IEEE Int. Conf. on *Image Processing,* ICIP'2005, **3**, pp. 305-308, Genoa, September 2005.
12. H. Wang, J. Peng, W. Wu, *Fusion algorithm for multisensor images based on discrete multiwavelet transform*, IEE Proc.-Vis. Image Signal Process., **149**, *5*, pp. 283-289, October 2002.

13 F. Argenti, L. Alparone, *Speckle removal from SAR images in the undecimated wavelet domain*, IEEE Trans. Geosci. Remote Sensing **40,** *11*, pp. 2363–2374, 2002.

14. A. Achim, E. Kuruoglu, J. Zerubia, *SAR Image Filtering Based on the Heavy-Tailed Rayleigh Model*, INRIA Rapport, N° 5493, February 2005.
15. S. Moga, A. Isar, *SONAR Image Denoising Using a Bayesian Approach in the Wavelet Domain,* Proceedings of International Conference *ASMDA 2007*, pp. 1275-1281, Chania, Crete, Greece, May 29–June 1, 2007.
16. M. Walessa, M. Datcu, *Model-Based Despeckling and Information Extraction from SAR Images*, IEEE Transactions on Geoscience and Remote Sensing, **38**, *5*, pp. 2258- 2269, September 2000.
17. M. Miller, N. Kingsbury, *Image Denoising Using Derotated Complex Wavelet Coefficients*, IEEE Transactions on Image Processing, **17**, *9*, pp. 1500-1511, September 2008.